

Paper presented at the IEEE 1986 Nuclear  
Science Symposium, October 29-31, 1986,  
Washington, DC

BNL 38861

To be published in IEEE Transactions on  
Nuclear Science, February 1987

BNL--38861

DE87 003207

**GAIN REDUCTION DUE TO SPACE CHARGE AT HIGH COUNTING RATES  
IN MULTIWIRED PROPORTIONAL CHAMBERS**

**G. C. Smith**

**Instrumentation Division, Brookhaven National Laboratory, Upton NY 11973-5000**

**and**

**E. Mathieson**

**Physics Department, Leicester University, Leicester LE1 7RH, England**

**October 1986**

**\*This research was supported in part by the U. S. Department of Energy:  
Contract No. DE-AC02-76CH00016.**

**DISTRIBUTION OF THIS DOCUMENT IS UNLIMITED**

G. C. Smith

Instrumentation Division, Brookhaven National Laboratory, Upton, NY 11973-5000

and

E. Mathieson

Physics Department, Leicester University, Leicester LE1 7RH, England

Abstract

Measurements with a small MWPC of gas gain reduction, due to ion space charge at high counting rates, have been compared with theoretical predictions. The quantity  $\ln(q/q_0)/(q/q_0)$ , where  $(q/q_0)$  is the relative reduced avalanche charge, has been found to be closely proportional to count rate, as predicted. The constant of proportionality is in good agreement with calculations made with a modified version of the original, simplified theory.

Introduction

Although gain reduction due to space charge at high counting rates is a well-studied phenomenon for coaxial chambers [1,2,3], only recently has a theoretical description been given for multiwire proportional chambers (MWPCs). [4] A very brief summary of a modified version of that treatment is given in the Appendix below. After making several simplifying assumptions, this analysis predicts that the relative reduced avalanche charge,  $q/q_0$ , should be related to the count rate per unit length per anode wire,  $n_1$ , by the expression

$$\ln(q/q_0) = -n_1 q / I_1 \quad (1)$$

The specific current constant,  $I_1$ , is given by

$$I_1 = I_m / k_m$$

where

$$I_m = 2\mu C_1 V_a / h^2 D \quad (2)$$

Here  $h$  is the anode-cathode spacing,  $\mu$  the positive ion mobility,  $V_a$  is the anode potential,  $C_1$  is the capacitance per unit length of anode wire, and

$$D = (1/M) dM/dV_a,$$

where  $M$  is the gas gain. The dimensionless factor,  $k_m(L/h)$ , which has a value between zero and unity, takes into account that only a finite length,  $L$ , of chamber is irradiated. The present theory differs from that of Ref. 4 in the calculation of this modifying factor (see Appendix). The number of anode wires irradiated may, for the present purposes, be assumed to be infinite (see next section).

The aim of this experiment was to compare measurements of  $q/q_0$ , in a small MWPC, with theoretical calculations from Eq. (1) so that the predictive value of this formula could be assessed.

Apparatus

The experimental arrangement is shown schematically in Fig. 1. The MWPC dimensions were anode-cathode spacing 3.00 mm, anode wire spacing 1.41 mm, anode wire diameter 8  $\mu$ m. There were thirteen normal anode wires with two larger diameter guard wires at each side. In order to simulate the situation in which an infinite number of anode wires are irradiated, observations were made only on the central wire, which was electrically isolated from the remainder. A detailed analysis shows

\*This research was supported in part by the U. S. Dept. of Energy: Contract No. DE-AC02-76CH00016.

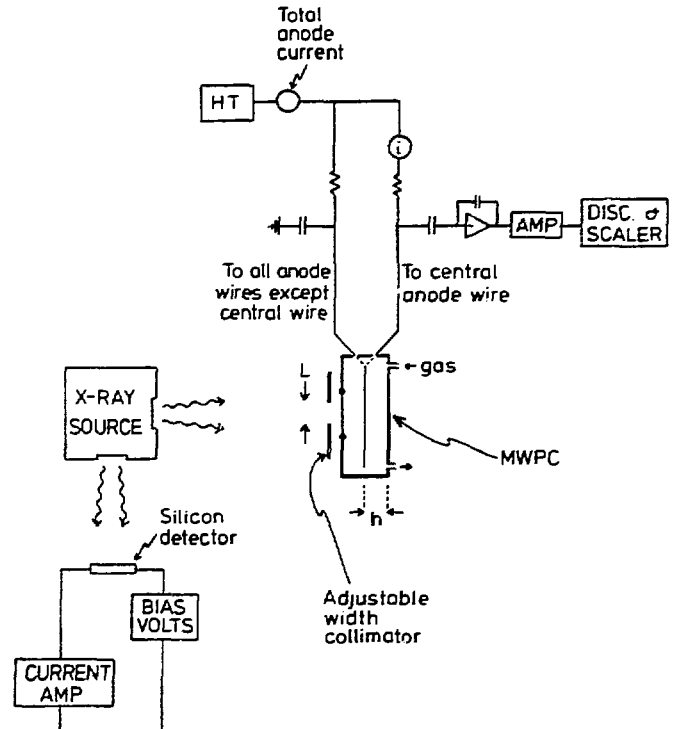


Fig. 1. Experimental arrangement, showing MWPC and silicon diode receiving radiation simultaneously from the x-ray source. The current from the central anode wire and the total anode current were measured separately.

that edge effects were therefore, for this geometry, negligible.

The fill gas was Xe/10%CO<sub>2</sub> flowing at atmospheric pressure and the anode voltage was 1640 V, yielding  $q_0$ , the low rate avalanche charge, as 0.16 pC. In Fig. 2 measurements of  $\ln(M)$  are plotted against  $V_a$ , showing that the relationship, over the full range of gain relevant to the present measurements, is practically linear; the slope of the straight line yields the value of  $D$ . A value for ion mobility was also derived in situ, by observing on an oscilloscope the minimum collection time at the cathodes for the positive ions. Knowing the chamber geometry and the field distribution, a value for  $\mu$  could be calculated.

The x-ray beam, from a copper target, was normal to the anode plane with the irradiated length of anode wire,  $L$ , defined by means of steel collimating shims. The x-ray intensity was continuously monitored by a silicon diode, placed at a constant position with respect to a second window of the x-ray tube. This diode was calibrated against the MWPC at very low count rates where lost counts were negligible. Linearity of the diode over the full range of x-ray intensities was accurately confirmed by calibrating it against an ionization chamber (in fact the MWPC with polarity reversed). The HT supply to the x-ray tube was smoothed to reduce the intensity modulation to

MASTER

## Experimental Results

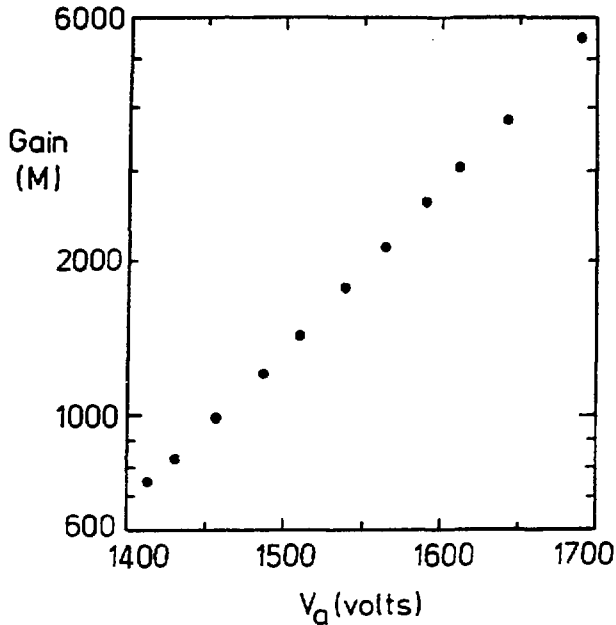


Fig. 2. The logarithm of gas gain plotted against anode voltage  $V_a$ . The slope of the best straight line gives  $D = (1/M)dM/dV_a = 0.00729/V$ .

about 8%. It is easily shown that this degree of modulation has no significant effect on the interpretation of Eq. 1.

Knowing the central anode wire current per unit length,  $i_1$ , and rate per unit length,  $n_1$ , the avalanche charge is simply obtained as  $q = i_1/n_1$ . This direct determination of  $q$  avoids the uncertainties introduced by pulse processing and pile-up.[2]

These are shown in Fig. 3, where  $\ln(q/q_0)$  has been plotted against central anode wire current density,  $i_1$ , for a range of values of irradiation length,  $L$ . It is seen that there is a very well-defined linear relationship over a large range of  $q/q_0$ ; the slopes of the straight lines give values for  $1/I_1$ . In Fig. 4 the experimental values of  $I_1$  are plotted against  $L/h$ . The continuous curve is the theoretical calculation, with  $k_m$  evaluated as described in the Appendix. The dashed line shows  $I_m = 223$  nA/cm, calculated from Eq. (2) with  $C_1 = 0.0519$  pF/cm (see Appendix 2 of Ref. 4) and  $\mu = 0.86$  cm<sup>2</sup>/Vs.

## Discussion

The marked linearity of the experimental points in Fig. 3 shows that the essential features of the theoretical model are realistic. Further, the good agreement over a wide range of  $L/h$  values between experimental and calculated values of  $I_1$  suggests that the initial assumptions are rather well justified. The value for ion mobility which appears in the expression for  $I_m$ , may seem rather high [5] but, as reported above, this value was derived in situ, from direct observation of ion collection time in the chamber. It is possible that some contaminant was present but, if so, its composition was very stable throughout the experiments. The sensitivity of ion mobility to small changes in gas composition is well known so that the predictive value of Eq. (1) may well be determined finally, in practice, by accuracy of knowledge of ion mobility in the chamber.

An important feature revealed by the present experimental work is that the special simplification contained in the original theory (see Appendix), although leading quickly to general, simple results, is not acceptable if accurate prediction at small  $L/h$  values.

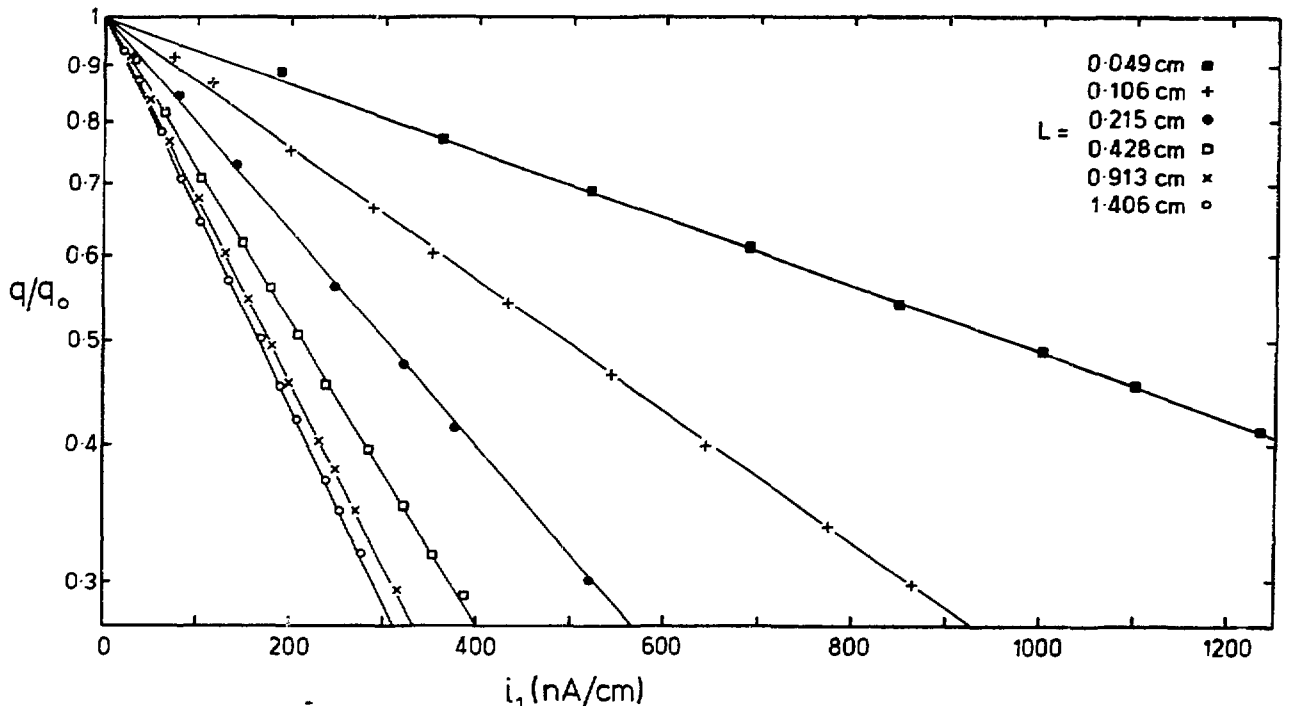


Fig. 3. Values of  $\ln(q/q_0)$  plotted against central anode wire current per unit length  $i_1$ , for various values of irradiated chamber length,  $L$ . The slopes of the straight lines yield experimental values for the quantity  $1/I_1 = k_m(L/h)/I_m$ . (Data for  $L = 0.537, 0.708,$  and  $1.067$  cm are not shown in order to avoid overcrowding, but are included in Fig. 4). Note that for the horizontal axis  $1000$  nA/cm  $\equiv 1$  pC.nHz/cm.

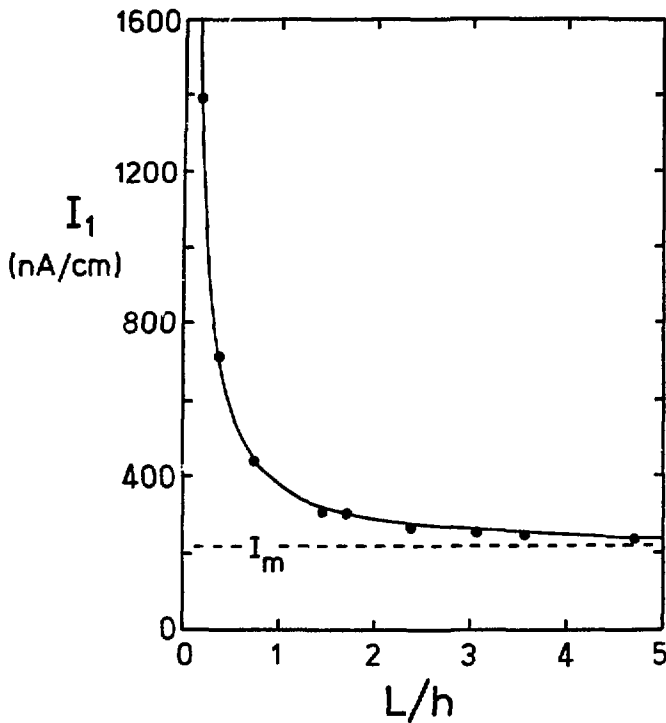


Fig. 4. Experimental values of  $I_1$  compared with theoretical prediction (continuous curve). As  $L/h \rightarrow 0$  the theoretical curve has the approximate form  $I_m/(1.05L/h)$ . The dashed line shows the value of  $I_m$ .

is required. There is, of course, a penalty for this accuracy in the increased complexity of the calculations. For some applications precise knowledge of gain reduction may not be necessary so that the original, simpler version would then be an adequate guide.

A fuller account of this work, including results of measurements with other gas mixtures and a more detailed description of the theory, will be given elsewhere.

#### Acknowledgements

The authors acknowledge helpful discussions with J. Fischer and V. Radeka. Much of the experimental hardware was skillfully constructed by E. Von Achen.

#### Appendix

Several simplifying assumptions must be made in order to develop for MWPCs a tractable theory of avalanche charge/count rate dependence; for brevity, discussions of these have been omitted below since they are examined in Ref. [4]. However, an important oversimplification introduced in [4] has now been removed in the present theoretical treatment.

Consider first a symmetrical multiwire chamber with count rate per wire per unit length  $n_1 =$  (constant) and with avalanches distributed uniformly in angle round the wires. Then it follows [4] that the space-charge density,  $\rho$ , is independent of position and given by

$$\rho = \frac{n_1 q \epsilon_0}{\mu V_a C_1} \quad (A1)$$

where  $q$  is the avalanche charge,  $\mu$  is the positive ion mobility,  $V_a$  is the anode voltage and  $C_1$  is the capacitance per unit length of anode wire.

Now consider in the chamber a very thin sheet of space charge, normal to the anode wire direction, of uniform density,  $\rho$ , given by the expression above, of thickness  $dx$  and of effectively infinite height. Then it may be shown [4] that the potential in the anode plane, in the absence of anode wires, at distance  $x$  from this sheet, is given by

$$\delta V(x) = n_1 q R_m \eta_m(x/h) \frac{dx}{h} \quad (A2)$$

Here  $h$  is the anode-cathode spacing,  $R_m = h^2/(2\mu V_a C_1)$  and  $\eta_m(x/h)$  is a dimensionless function defined by the integral,

$$\eta_m(z) = \frac{2}{\pi^2} \int_0^{+\pi/2} \ln \left( \frac{\cosh(\pi z/2) + \cos \theta}{\cosh(\pi z/2) - \cos \theta} \right) d\theta \quad (A3)$$

Since the anode wire surfaces must be equipotentials, induced charges, of linear density  $\sigma(x)$  must produce a cancelling distribution  $-\delta V(x)$ . The space-charge field distribution at the anode wire surfaces due to these induced line charges may conveniently be expressed in terms of an effective anode voltage distribution  $-\delta V_e(x)$ . In the original theoretical treatment [4] it has been assumed that  $\delta V_e = \delta V$ , an approximation which greatly simplifies the subsequent analysis and leads to approximate but general results. However for a more accurate treatment the real relationship between  $\delta V_e$  and  $\delta V$  must be found. This is achieved as shown, in summary, below.

Electrostatic image theory allows one to write an expression for  $\delta V(x)$  in terms of the (unknown) induced line charge density  $\sigma(x)$ . However, before giving this expression it is convenient to change functions in the following manner. The effective anode voltage distribution can be expressed in terms of line charge density as  $\delta V_e(x) = \sigma(x)/C_1$  and then, in view of Eq. (A2), it is sensible to define a new "effective" function  $\eta_{me}(x/h)$  by

$$\delta V_e(x) = n_1 q R_m \eta_{me}(x/h) \frac{dx}{h} \quad (A4)$$

Then in terms of  $\eta_m$  and  $\eta_{me}$ , instead of  $\delta V$  and  $\sigma$ , the expression, from image theory, for potential may be written

$$\eta_m(x/h) = C \int_{-\infty}^{\infty} \sum_n \sum_k \frac{\cos(\pi n) \eta_{me}(x'/h)}{\{a^2 + ((x-x')/h)^2\}^{1/2}} \frac{dx'}{h} \quad (A5)$$

Here  $C = C_1/4\pi\epsilon_0$  and  $a^2 = (r_a/h)^2 + (2n)^2 + (ks/h)^2$ . The summations are over  $n$  and  $k$  from  $-\infty$  to  $+\infty$ .  $r_a$  is the anode wire radius and  $s$  is the anode wire spacing.

Recognizing that Eq. (A5) is a convolution integral, it follows that the unknown function  $\eta_{me}$  can be found (numerically) as the inverse Fourier transform of  $G(\omega)/H_0(\omega)$  where  $G(\omega)$  is the transform of  $\eta_m(x/h)$  and  $H_0(\omega)$  is the transform of

$$C \sum_n \sum_k \frac{\cos(\pi n)}{\{a^2 + (x/h)^2\}^{1/2}}$$

It can be shown that

$$H_0(\omega) = C \sum_n \sum_k 2 \cos(\pi n) K_0(a\omega) \quad (A6)$$

where  $K_0$  is the zero order modified Bessel function of the second kind. It should be noted that particular care is necessary in the numerical evaluation of  $H_0(\omega)$ , see Ref. 6. An important check on the final evaluation of  $\eta_{me}$  is the requirement that

$$\int_{-\infty}^{\infty} \eta_{me}(z) dz = 1 \quad (A7)$$

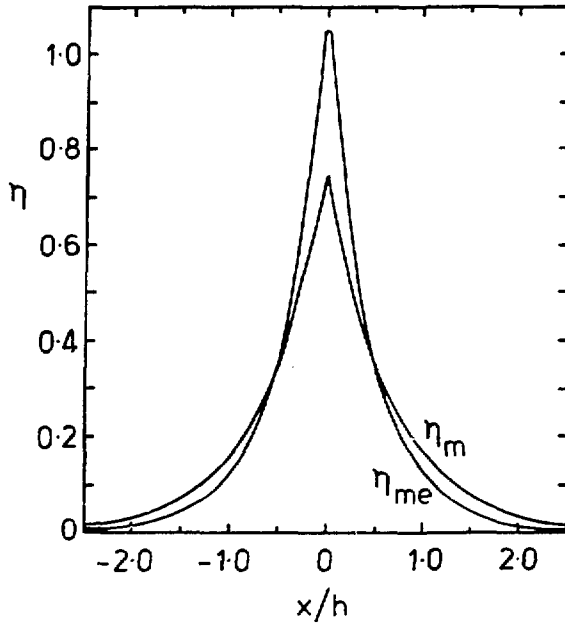


Fig. 5. The dimensionless function  $\eta_{me}(x/h, r_a/h, s/h)$  shown as a function of  $x/h$ , with  $r_a/h = 1.33 \times 10^{-3}$  and  $s/h = 0.470$ . Also shown is the simpler function  $\eta_m(x/h)$ .

The functions  $\eta_m(x/h)$  and  $\eta_{me}(x/h, r_a/h, s/h)$ , for a particular value of  $r_a/h$  and  $s/h$ , are shown in Fig. 5.

Thus, finally, for uniform irradiation over a finite length of chamber we may therefore write for the effective anode voltage distribution

$$\delta V_e(x) = n_1 R_m \int_{-L/2}^{+L/2} q(x') \eta_{me}((x-x')/h) \frac{dx'}{h} \quad (A8)$$

Now over a considerable range of gas gain  $M$ , for most chamber geometries and gas mixtures, there is a linear relationship between  $\ln(M)$  and  $V_a$  (see Fig. 2). That is,  $D = (1/M)dM/dV_a$  is practically a constant and therefore, if  $q_0$  is the avalanche charge at zero count rate, we may write

$$\ln \frac{q(x)}{q_0} = -D \delta V_e(x) \quad (A9)$$

If we now assume, reasonably, that  $q(x')$  may be replaced in the integrand in Eq. (A8) by its average value  $q$  then

$$\ln \frac{q}{q_0} = -\frac{n_1 q}{I_m} k_m(L/h) \quad (A10)$$

## DISCLAIMER

This report was prepared as an account of work sponsored by an agency of the United States Government. Neither the United States Government nor any agency thereof, nor any of their employees, makes any warranty, express or implied, or assumes any legal liability or responsibility for the accuracy, completeness, or usefulness of any information, apparatus, product, or process disclosed, or represents that its use would not infringe privately owned rights. Reference herein to any specific commercial product, process, or service by trade name, trademark, manufacturer, or otherwise does not necessarily constitute or imply its endorsement, recommendation, or favoring by the United States Government or any agency thereof. The views and opinions of authors expressed herein do not necessarily state or reflect those of the United States Government or any agency thereof.

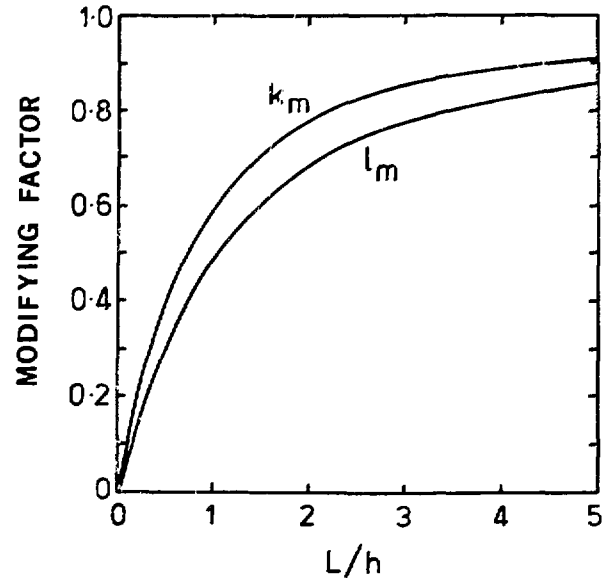


Fig. 6. The modifying factor  $k_m(L/h, r_a/h, s/h)$  shown as a function of  $L/h$  with  $r_a/h = 1.33 \times 10^{-3}$  and  $s/h = 0.470$ . For this geometry, as  $L/h \rightarrow 0$ ,  $k_m$  has the approximate value  $1.05L/h$ . Also shown is the simpler factor  $l_m(L/h)$ .

where  $I_m = 1/(D \cdot R_m)$  and  $k_m(L/h)$  is the average value of the integral. That is

$$k_m(L/h) = \frac{h}{L} \int_{-L/2h}^{+L/2h} \eta_{me}(z-z') dz' dz \quad (A11)$$

The factor  $k_m(L/h, r_a/h, s/h)$ , which is shown in Fig. 6, should replace for accurate predictions at small  $L/h$  the simpler modifying factor  $l_m(L/h)$  introduced in Ref. 4. Note that, unlike  $l_m$ ,  $k_m$  is a function of chamber geometry  $r_a/h$  and  $s/h$ .

## References

1. R. W. Hendricks, Rev. Sci. Instrum. 40 (1969) 1216.
2. H. Sipila and V. Vanha-Honko, Nucl. Instrum. & Meth. 153 (1978) 461.
3. H. Sipila, V. Vanha-Honko, and J. Berquist, Nucl. Instrum. & Meth. 176 (1980) 381.
4. E. Mathieson, Nucl. Instrum. & Meth. A249 (1986) 413.
5. E. W. McDaniel and E. A. Mason, Mobility and Diffusion of Ions in Gases, Wiley, New York (1973).
6. J. R. Thompson, J. S. Gordon, and E. Mathieson, Nucl. Instrum. & Meth. A234 (1985) 505.